Supplementary Information

Converting pyrolysis carbon black derived from waste tires into highly efficient adsorbent for dye wastewater

Wenli Liu[a], Pei Chen[b], Yanzhi Sun[a,*], Chuanjin Huang[c], Yongmei Chen[a], Jun Guo[c], Junqing Pan[b] and Pingyu Wan[a]

[a]National Fundamental Research Laboratory of New Hazardous Chemicals Assessment and Accident Analysis, Institute of Applied Electrochemistry, Beijing University of Chemical Technology, Beijing 100029, China

[b]State Key Laboratory of Chemical Resource Engineering, Beijing University of Chemical Technology, Beijing 100029, China

[c]China Chemical Equipment Technology Co., LTD, Shanghai 201403, China

*E-mail: sunyz@buct.edu.cn (Y. Sun)

Tel./Fax: 8610-64435452

1. The plausible reaction mechanism during KOH activation

$$2C+6KOH \rightarrow 2K+2K_2CO_3+3H_2$$

$$K_2CO_3 \rightarrow K_2O+CO_2$$

$$K_2CO_3+2C \rightarrow 2K+3CO$$

$$CO_2+C \rightarrow 2CO$$

$$CO+H_2O \rightarrow CO_2+H_2$$

$$C+H_2O \rightarrow CO+H_2$$

$$ZnO+4KOH \rightarrow K_2Zn(OH)_4+K_2O$$

$$ZnS+2KOH \rightarrow Zn(OH)_2+K_2S$$

$$Zn(OH)_2+2KOH \rightarrow K_2Zn(OH)_4$$

$$SiO_2+2KOH \rightarrow K_2SiO_3+H_2O$$

$$2Zn^{2+}+SiO_3^{2-}+2OH^- \rightarrow Zn_2SiO_4+H_2O$$

$$2CaCO_3+SiO_2 \rightarrow Ca_2SiO_4+2CO_2$$

$$3CaCO_3+28.5Fe_2O_3 \rightarrow 20Ca_{0.15}Fe_{2.85}O_4+3CO_2+4.25O_2$$

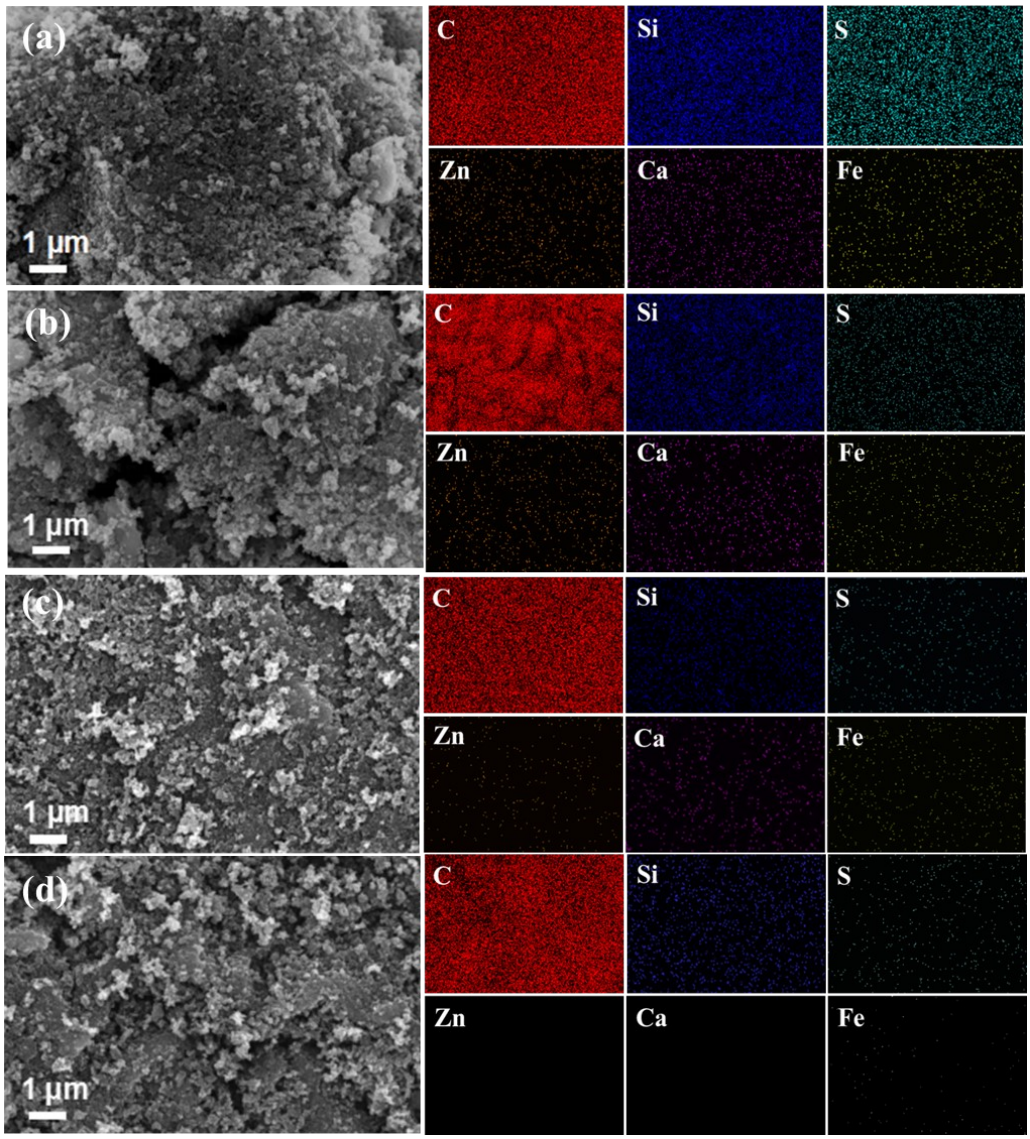

Fig. S1. SEM and corresponding EDS images of (a) CBp, (b) CBph, (c) ACBp, (d) ACBph

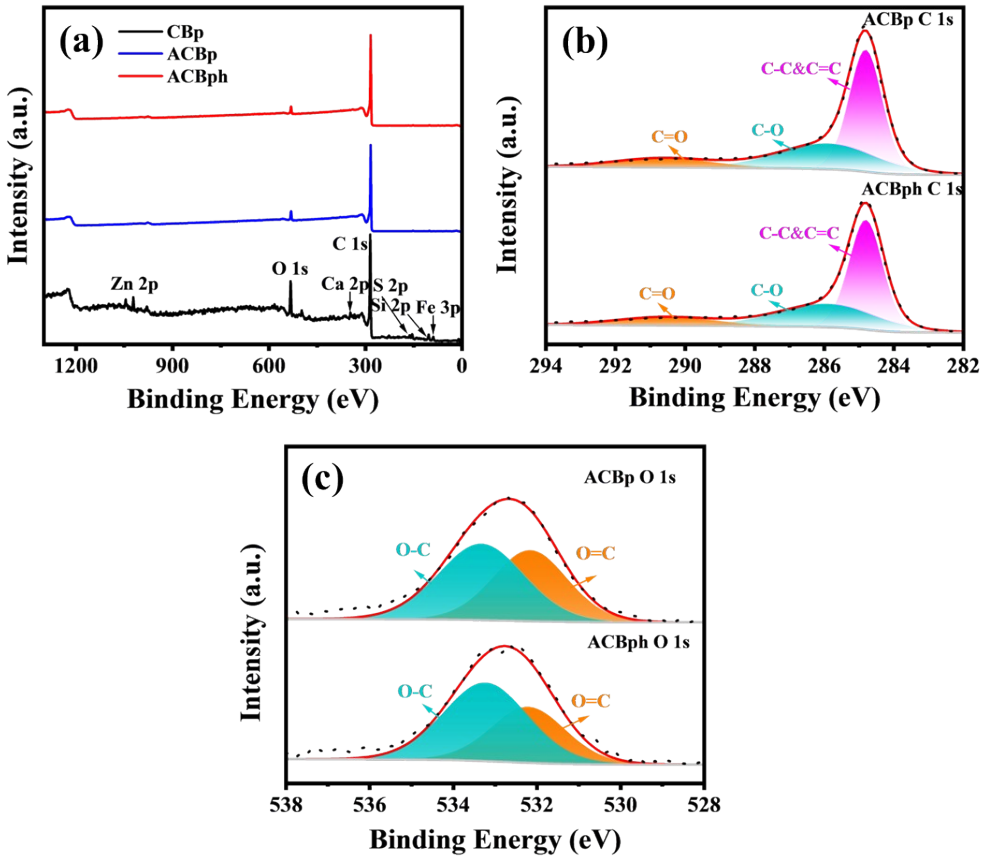

Fig. S2. (a) XPS spectra of CBp, ACBp and ACBph; (b) C1s spectra of ACBp and ACBph; (c) O1s spectra of ACBp and ACBph

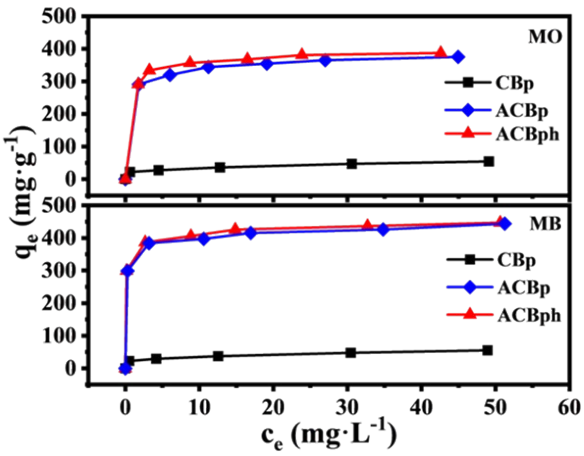

Fig. S3. q_e of MO and MB by different adsorbents (Adsorption conditions: initial $c_{MO} = c_{MB} =$ 40 - 140 mg·L^{-1}, $c_{adsorbent} = 0.2$ g·L^{-1}, pH = 3.0 (MO) or 10.0 (MB), T = 25 °C, t = 3 h)

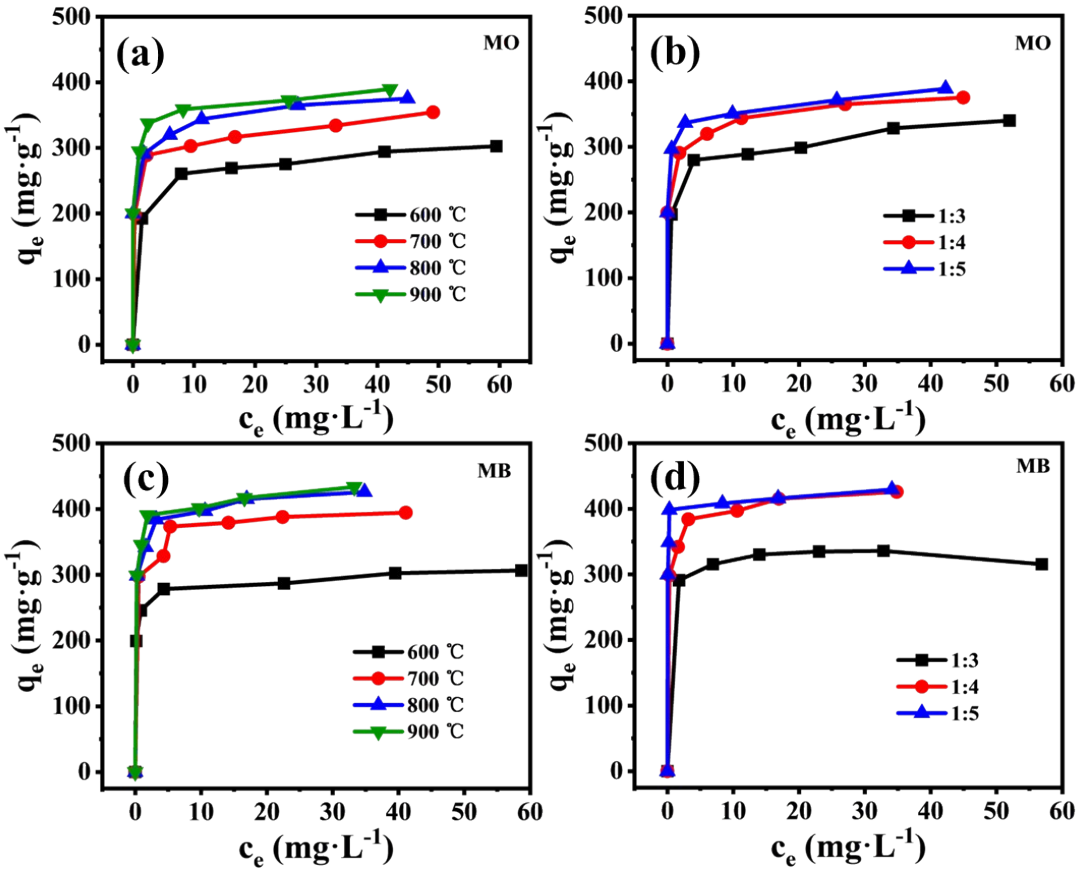

Fig. S4. Effect of ACBp prepared under different activation conditions on adsorption of MO and MB: (a, c) different temperatures, (b, d) different ratios (Adsorption conditions: initial $c_{MO} = c_{MB} = 40 - 140$ mg·L^{-1}, $c_{adsorbent} = 0.2$ g·L^{-1}, pH = 3.0 (MO) or 10.0 (MB), T = 25 °C, t = 3 h)

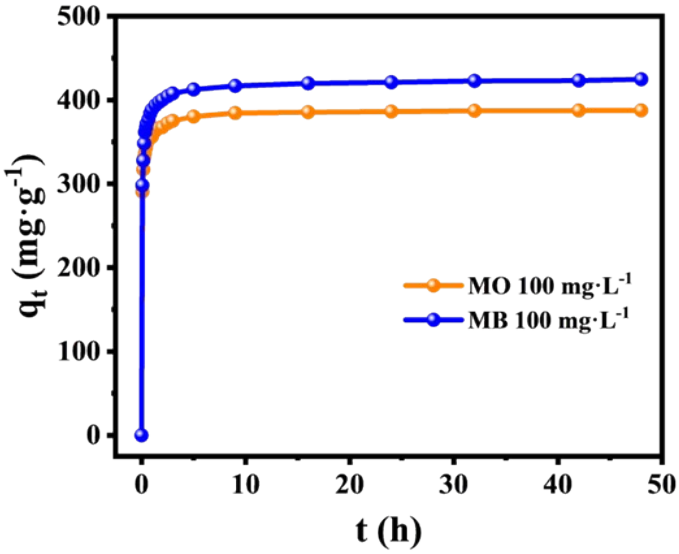

Fig. S5. Time on the adsorption capacity at pH = 3.0 (MO) and 10.0 (MB) (initial $c_{MO} = c_{MB} = 100$ mg·L^{-1}, $c_{adsorbent} = 0.2$ g·L^{-1}, T = 25 °C)

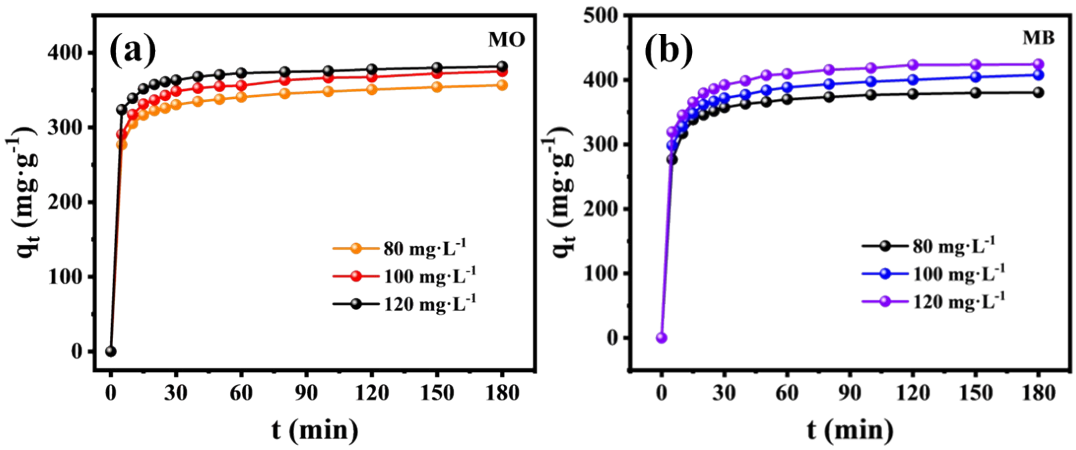

Fig. S6. The adsorption capacity curve of ACBp for (a) MO and (b) MB over time at different concentrations (Adsorption conditions: initial $c_{MO} = c_{MB} = 80$, 100 and 120 mg·L^{-1}, $c_{adsorbent} = 0.2$ g·L^{-1}, pH = 3.0 (MO) or 10.0 (MB), T = 25 °C, t = 3 h)

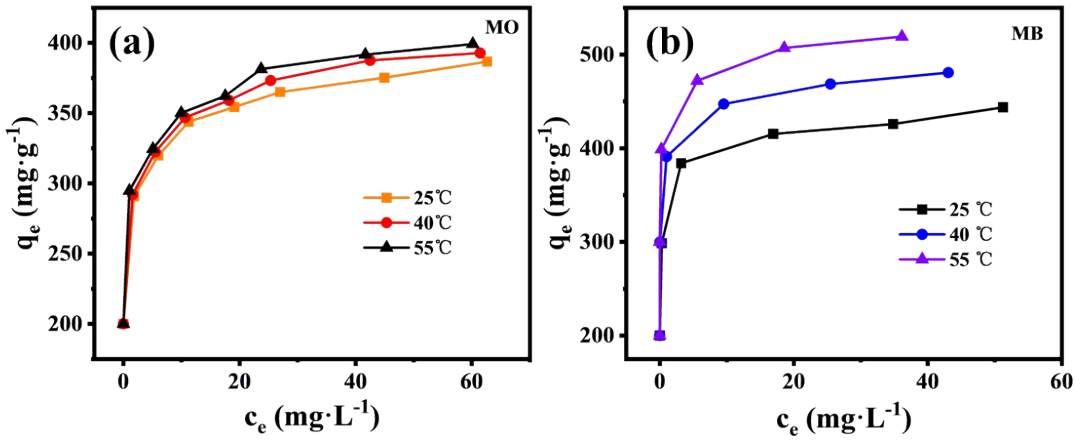

Fig. S7. The adsorption capacity curves of ACBp on (a) MO and (b) MB at different temperatures (Adsorption conditions: initial $c_{MO} = c_{MB} = 40$ - 140 mg·L^{-1}, $c_{adsorbent} = 0.2$ g·L^{-1}, pH = 3.0 (MO) or 10.0 (MB), T = 25 - 55 °C, t = 3 h)

Table S1 The detailed information of characterization and measurement instruments

Instruments	Instrument model	Company/Country	Conditions
Scanning electron microscopy (SEM)	Supra 55	ZEISS/Germany	Operating voltage of 15 kV
Energy Dispersive Spectroscopy (EDS)	Supra 55	ZEISS/Germany	Operating voltage of 15 kV
X-ray diffraction (XRD)	UItimaI II	Rigaku Co./Japan	2θ ranging from 5-90° with Cu Kα radiation at scan of 10° min^{-1}
Fourier transform infrared spectrometer (FTIR)	TENSOR II	Bruker/Germany	Wave number, 4000-500 cm^{-1}
Raman spectroscopy	LabRAM Aramis	HORIBA Jobin Yvon S.A.S/France	Wavelength, λ = 514 nm
Laser Particle Size Analyzer	Mastersizer 3000	Malvern Panalytical/English	Operating temperature, + 5 °C - + 40 °C
Contact angle	K100	Kruss/Germany	
Nitrogen adsorption and desorption isotherm (BET)	Autosorb iQ	Quantachrome Instruments/USA	At 77 K
X-ray photoelectron spectroscopy (XPS)	K-Alpha	Thermo Fisher Scientific/USA	Al Kα radiation (1486.6 eV)
Potentiometric Hydrogen Ion Concentration Meter (pH-meter)	FE28	Mettler Toledo Co., Ltd./China	pH = 1-14
Ultraviolet-visible spectrophotometer (UV/Vis)	UV-2550	Shimadzu/Japan	Wavelength, λ = 190-900 nm

Table S2 Kinetic model, isotherm model and thermodynamic equations for MO and MB adsorption

Equation		
$$q_e = \frac{(c_0 - c_e)V}{m}$$		Eq.(1)
$$Removal = \frac{c_0 - c_e}{c_0} \times 100\%$$		Eq.(2)
Kinetic models	**Linearized Equation**	**Reference**
Pseudo-first-order kinetics	$\ln (q_e - q_t) = \ln q_e - k_1 t$ Eq.(3)	[1]
Pseudo-second-order kinetics	$\frac{t}{q_t} = \frac{1}{k_2 \times q_e^2} + \frac{t}{q_e}$ Eq.(4)	[2]
Intra-particle diffusion model	$q_t = k_{id} \times t^{1/2} + c_{id}$ Eq.(5)	[3]
Isotherm models	**Linearized Equation**	**Reference**
Langmuir	$\frac{c_e}{q_e} = \frac{c_e}{q_m} + \frac{1}{K_L q_m}$; $R_L = \frac{1}{1 + K_L c_0}$ Eq.(6)	[4]
Freundlich	$lnq_e = lnK_F + \frac{1}{n_F} lnc_e$ Eq.(7)	[5]
Temkin	$q_e = BlnK_T + Blnc_e$; $B = \frac{RT}{b}$ Eq.(8)	[6]
Thermodynamics	**Equation**	**Reference**
	$lnK_c = \frac{\Delta S}{R} - \frac{\Delta H}{RT}$ Eq.(9)	[7]
	$\Delta G = -RTlnK_c$ Eq.(10)	
	$\Delta G = \Delta H - T\Delta S$ Eq.(11)	
	$K_c = \frac{q_e}{c_e}$ Eq.(12)	

where c_0 (mg·L^{-1}) is the initial dye concentration, with consideration of

experimental factors such as sorption on the flask, separation losses, and volatilization (referred to as $c_{control}$), c_e (mg·L^{-1}) is the equilibrium liquid-phase concentration after adsorption, q_e (mg·g^{-1}) is the equilibrium adsorption amount, q_t (mg·g^{-1}) is the adsorption amount at time t (min), q_m (mg·g^{-1}) is the maximum adsorption amount, k_1 (min^{-1}) is the pseudo-primary model kinetic rate constant, k_2 (g·mg^{-1}·min^{-1}) is the pseudo-secondary model kinetic rate constant, k_{id} (mg·g^{-1}·min$^{-1/2}$) is the intra-particle diffusion rate constant, c_{id} (mg·g^{-1}) is the intra-particle diffusion constant ; K_L (L·mg^{-1}) and R_L are Langmuir constants and separation factors, K_F (mg·g^{-1}) and n_F are Freundlich constants, K_T (L·g^{-1}) and B are Temkin constants, and b (J·mol^{-1}) is a constant related to the heat of adsorption constant associated with the heat of adsorption; R = 8.314 J·mol^{-1}·K^{-1} is the universal gas constant, T (K) is the absolute temperature, K_c (L·mg^{-1}) is the thermodynamic equilibrium constant, the parameters ΔH (kJ·mol^{-1}) and ΔS (J·mol^{-1}·K^{-1}) are calculated from the slope and intercept of the lnK_c versus 1/T curve, and ΔG (kJ·mol^{-1}) is calculated based on ΔH and ΔS are calculated.

Table S3 Elemental content of carbon black samples

Sample	C (at%)	O (at%)	Si (at%)	S (at%)	Zn (at%)	Ca (at%)	Fe (at%)
CBp	87.09	8.95	2.03	1.24	0.52	0.12	0.05
CBph	90.77	6.50	2.38	0.26	0.03	0.04	0.02
ACBp	89.86	9.30	0.22	0.36	0.12	0.10	0.04
ACBph	93.29	6.51	0.11	0.03	0.01	0.04	0.01

(Note: at% refers to atomic percentage.)

Table S4 BET data of carbon black samples

Sample	S_{BET}	Pore Volume	V_{micro}（cm^3·g	V_{non-}	Average pore size

	(m²·g⁻¹)	(cm³·g⁻¹)	⁻¹)	micro（cm³·g⁻¹）	(nm)
CBp	49	0.46	0	0.46	37.44
ACBp	789	0.74	0.25	0.49	3.74
ACBph	808	0.86	0.26	0.60	4.28

Table S5 Yields of ACBp under different activation conditions

Reaction conditions	600 °C 1:4	700 °C 1:4	800 °C 1:4	900 °C 1:4	800 °C 1:3	800 °C 1:5
***Y* (%)**	56.67	51.80	50.93	43.33	55.60	42.47

Table S6 Parameters of the nonlinear PFO, PSO, and IPD kinetic models

Kinetic model	**Parameter**	**MO 80 mg·L⁻¹**	**MO 100 mg·L⁻¹**	**MO 120 mg·L⁻¹**	**MB 80 mg·L⁻¹**	**MB 100 mg·L⁻¹**	**MB 120 mg·L⁻¹**
Pseudo-first-order kinetics	k_1 (min⁻¹)	0.015	0.019	0.021	0.031	0.021	0.033
	q_e (mg·g⁻¹)	14.1	12.0	40.8	73.9	80.8	100.9
	R^2 (%)	92.8	92.6	94.6	97.5	96.4	96.6
Pseudo-second-order kinetics	k_2 (mg·mg⁻¹·min⁻¹)	1.11	1.04	1.70	1.13	0.79	2.32
	q_e (mg·g⁻¹)	359.7	377.4	383.1	384.6	411.5	431.0
	R^2 (%)	99.9	99.9	99.9	99.9	99.9	99.9
Intra-particle diffusion model	K_{id1} (mg·g⁻¹·min⁻¹/²)	24.55	25.04	17.03	38.02	30.51	28.26
	C_{id1} (mg·g⁻¹)	223.63	235.66	285.44	193.08	230.45	255.96
	R2 1 (%)	94.46	98.08	99.91	97.90	99.80	99.99
	K_{id2} (g·mg⁻¹·min⁻¹/²)	5.50	5.74	4.62	7.16	8.07	9.31
	C_{id2} (mg·g⁻¹)	298.87	314.10	337.73	315.78	326.43	339.45
	R2 2 (%)	97.33	87.14	98.18	95.84	99.29	97.52

	K_{id3} ($g \cdot mg^{-1} \cdot min^{-1/2}$)	2.52	2.66	1.69	1.50	3.20	1.97
	C_{id3} ($mg \cdot g^{-1}$)	322.94	339.38	359.08	361.10	365.00	399.08
	R2 3 (%)	99.75	97.91	98.92	89.47	99.76	77.02

Table S7 Parameters of adsorption isotherms at different temperatures

		MO			MB		
Langmuir	T (K)	273.15	288.15	328.15	273.15	288.15	328.15
	q_m ($mg \cdot g^{-1}$)	390.6	400.0	404.9	444.4	485.4	523.6
	95% CI	(386.7, 394.5)	(395.7, 404.3)	(401.5, 408.3)	(441.1, 447.7)	(481.0, 489,8)	(519.8, 527.4)
	K_L ($L \cdot mg^{-1}$)	0.694	0.716	0.774	1.286	1.791	2.732
	R_L	0.018	0.017	0.016	0.008	0.006	0.004
	R^2 (%)	99.9	99.9	99.9	99.9	99.9	99.9
Freundlich	K_F ($mg^{1-1/n} \cdot L^{1/n} \cdot g^{-1}$)	278.66	281.55	291.51	335.29	391.97	362.12
	$1/n_F$	0.080	0.084	0.078	0.073	0.055	0.049
	R^2 (%)	99.1	99.2	98.3	95.2	99.5	96.5
Temkin	B	27.07	28.73	27.05	26.72	23.94	24.08
	K_T ($L \cdot g^{-1}$)	25.38	15.58	43.34	311.60	12684.6	66094.8
	b ($J \cdot mol^{-1}$)	91.57	83.38	100.84	92.79	100.09	113.28
	R^2 (%)	99.4	99.3	97.7	96.7	99.8	99.7

References

[1] S. Lagergren, *Kungliga Svenska Vetenskapsakademiens Handlingar*, 1898, **24**, 1-39.

[2] Y. S. Ho and G. McKay, *Process Biochemistry*, 1999, **34**(5), 451-465.

[3] W. J. Weber Jr and J. C. Morris, *Journal of the Sanitary Engineering Division*,

1963, **89**(2), 31-59.

[4] I. Langmuir, *Journal of the American Chemical Society*, 1918, **40**(9), 1361-1403.

[5] H. Freundlich, *Zeitschrift Für Physikalische Chemie*, 1907, **57**(1), 385-470.

[6] M. I. Temkin, *Acta Physiochimica URSS*, 1940, **12**, 327-356.

[7] W. Rudzinski and D. H. Everett, *Academic Press*, 2012.